

Continuing Studies of the Hercules Thick Disk Cloud

Aaron Haviland and Jeffrey A. Larsen (United States Naval Academy)

R. M. Humphreys (University of Minnesota) and J. E. Cabanela (Minnesota State University, Moorhead)

Abstract

Larsen and Humphreys (1996) discovered an excess in faint blue stars in the inner part of the Galaxy when comparing POSS I star counts between Q1 and Q4. This excess was explored further in Parker et al. (2004) and was confirmed by Juric et al. (2008) using SDSS data. The excess comprises a population of stars which could be due to an interaction with the disk bar, a triaxial thick disk or a merger remnant/stream but is difficult to study because of the large amounts of quality star counts in Q1 and Q4 required above and below the Galactic plane. In this work we continue our analysis by presenting new data from our program of wide field photometric and spectroscopic observations taken from Kitt Peak and CTIO. Using photometric parallax and Galactic models we attempt to understand this population's origin and extent.

Introduction

The Hercules Thick Disk Cloud was first discovered in 1996 when Larsen and Humphreys observed an excess in paired field star counts about the center of the Galaxy at $l = 30^\circ$, 40° . They calculated a 25-30% excess in the number of faint blue stars at $l = 20^\circ$ 45' in Quadrant 1 (Q1) of the Galaxy compared to the complementary fields in Quadrant 4 (Q4).

To map the extent and shape of the asymmetric distribution and further identify the contributing stellar population, Parker, Humphreys and Larsen (2003) greatly extended the search to 40 contiguous fields from the digitized POSS I (Cabanela et al. 2003) on each side of the Sun-Center line plus the same number of fields below the plane in Q1. They examined the star count ratio for paired fields in three color ranges: blue, intermediate and red. Halo and thick disk stars dominate the blue color bin; thick disk stars make a significant contribution to the intermediate color range and fainter than 17th magnitude they are comparable to the number of disk stars. The red band is almost exclusively composed of old disk stars. Over 6 million stars were used in the star count analysis.

They found a 25% excess in the number of probable thick disk stars in Q1, $l = 20^\circ$ to 60° and 20° to 40° above and below the plane compared to the complementary fields ($l = 340^\circ$ to 300°) in Q4. While the region of the asymmetry is somewhat irregular in shape, it is also fairly uniform and covers several hundred square degrees. It is therefore a major substructure in the Galaxy due to more than smallscale clumpiness. Assuming that these are primarily main sequence thick disk stars, they are 1-2 kpc from the Sun and about 0.5 to 1.5 kpc above (and below) the plane.

Parker et al. (2004) also found an associated kinematic signature. Using velocities from spectra for over 700 stars obtained with Hydra on WIYN and the CTIO 4-m. Not only is the v_z distribution asymmetric, but the thick disk stars in Q1 have a much slower effective rotation rate ω compared to the corresponding Q4 stars. A solution for the radial and tangential components of the v_z velocity reveals a significant lag 80 to 90 kpc in the direction of Galactic rotation for the thick disk stars in Q1.

The recent release of the SDSS Data Release 5 (DR5) photometry in Q1 led to the discovery of an unrelated feature at much fainter magnitudes, the distant Hercules-Aquila cloud (Belokurov et al. 2007) as well as confirming our asymmetry in the inner Galaxy through the comprehensive photometric parallax study by Juric et al. (2008). The SDSS survey is not a good probe of the thick disk inside the Solar orbit since it extends below $b = 30^\circ$ in only a few directions in Q1 and has only limited coverage in Q4. Larsen et al. (2008) presented APS star count data that eliminated the possibility that the feature is a ring.

In 2008, Larsen and Humphreys named this Galactic substructure the Hercules Thick Disk Cloud and this poster presents our initial efforts to discern the nature of this cloud.

Possible Origins and Signatures of the Hercules Thick Disk Cloud

- FOSSIL REMNANT OF A MERGER:** A fossil remnant of a merger can cause an asymmetry in star counts. In our data this feature would be of a relatively confined spatial extent, similar to other tidal debris fields seen for known satellites of the Milky Way.
- INTERACTION OF THICK DISK/INNER HALO STARS WITH THE ROTATING STELLAR BAR:** A rotating stellar bar in the disk could induce a gravitational wave (Hernquist and Weinberg 1992, Debattista and Sellwood 1998). Their models would appear in our data as an excess of stars in Q1 versus Q4 along the line of sight above and below the Galactic plane and a measurable lag in rotation in Q1. Because the bar is closer to the center of the Galaxy than us, we would not see the feature far from the Galactic Center.
- TRIAxIAL THICK DISK/INNER HALO:** A triaxial distribution, with its major axis in Q1, would be visible in our data as an excess of stars in Q1 versus Q4 along the line of sight above and below the Galactic plane extending Galactic longitudes very far from the Galactic Center.

Observations

We have begun a program of photometric and spectroscopic observations to map the size and extent of the asymmetry along our line of sight and to determine the degree of spatial and kinematic asymmetry above and below the plane. While this is not the entire program, it is sufficient to answer the first questions about the nature of the cloud. The primary data sources for the UBVRI photometric observations presented in this poster are the:

- Northern sky: 90-Prime Imager at Kitt Peak, AZ (May 2006, September 2006, May 2007, October 2007)
- Southern sky: 1.0-m SMARTS Consortium telescope at the Cerro Tololo Inter-American Observatory near La Serena, Chile (April 2006, October 2008).

In Figure 3 and Table 1, we present the distribution of our project fields on the sky and their relevant observational parameters. Observations were conducted so that the completeness limits were $V = 19$ at CTIO and $V = 21$ at KPNO and approximately 1 square degree was imaged for each field.



Figure 1. 1.0-m SMARTS Consortium telescope at Cerro Tololo.



Figure 2. 90 Prime imager on the Bok 90" telescope on Kitt Peak.

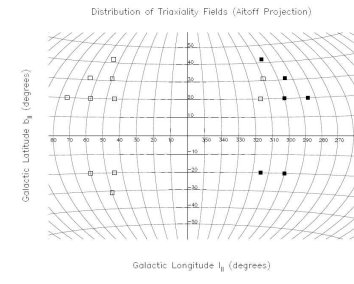


Figure 3. Distribution of program fields on the sky.

Table 1. Observational Circumstances of Project Fields. 90Prime fields are plotted as open squares, CTIO fields are plotted as filled squares. Symbol size is approximately correct for the area of each region.

Field Name	l	b	RA (J2000)	Dec (J2000)	Camera	Area	UT Date
TDA045+20	45°	+20°	15:49:25	+10:27:45	90Prime	1.02	29 May 2006
TDA050+31	50°	+31°	14:42:59	+19:16:12	90Prime	1.02	29 May 2006
TDA055+42	55°	+42°	15:29:19	+26:59:56	90Prime	1.02	30 May 2006
TDA060+20	60°	+20°	14:54:07	+17:10:33	90Prime	1.01	26 May 2006
TDA065+31	65°	+31°	14:41:23	+23:45:05	90Prime	1.01	26 May 2006
TDA075+20	75°	+20°	13:55:00	+22:53:09	90Prime	1.02	29 May 2006
TDA315+20	315°	+20°	21:27:15	-27:35:53	Y4KCam	0.92	7 Apr 2006
TDA310+31	310°	+31°	21:56:55	-21:37:43	Y4KCam	0.91	9 Apr 2006
TDA305+42	305°	+42°	22:26:07	-17:02:30	90Prime	1.02	27 May 2006
TDA300+20	300°	+20°	22:35:02	-28:38:08	Y4KCam	0.92	6 Apr 2006
TDA295+31	295°	+31°	23:00:07	-25:12:37	Y4KCam	0.89	7 Apr 2006
TDA285+20	285°	+20°	23:44:04	-28:28:19	Y4KCam	0.92	6 Apr 2006
TDA045-20	45°	-20°	14:34:08	-10:21:11	90Prime	1.02	31 May 2006
TDA050-31	50°	-31°	13:58:00	-09:28:21	90Prime	1.02	30 May 2006
TDA060-20	60°	-20°	14:01:29	-02:16:57	90Prime	1.02	29 May 2006
TDA315-20	315°	-20°	21:35:54	-55:32:43	Y4KCam	0.94	8 Apr 2006
TDA300-20	300°	-20°	23:03:01	-48:35:14	Y4KCam	0.96	8 Apr 2006

Analysis

For our initial studies we have decided to do a simple cut on an unambiguous feature of the color magnitude diagram which isolates stars in the thick disk/halo regions. Figure 4 shows an example color-magnitude diagram for one of our fields, B-V color versus V apparent magnitude. The green lines delineate the magnitude range in which all project fields are known to be complete.

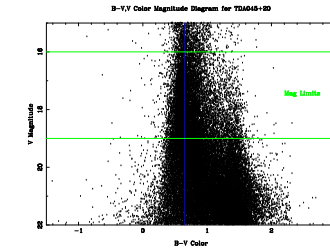


Figure 4. Color-magnitude diagram for TDA045+20, one of our project fields.

As with most field star color-magnitude diagrams the bimodal appearance is due to the galaxy having more than one component. Figure 5 shows the predictions of Larsen's GALM0D galaxy star count model for the same field. The model shows that the right lobe (fainter, redder stars with $B - V = 1.5$) is associated with relatively close dwarf stars in the disk of the galaxy while the left lobe ($B - V = 0.7$) represents hotter disk stars (for bright magnitudes) which at fainter magnitudes becomes mostly halo and thick disk stars.

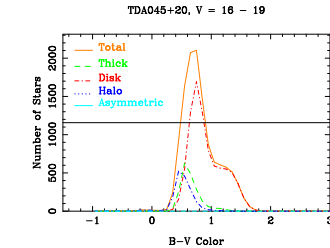


Figure 5. For stars between $V = 16$ and $V = 19$, GALM0D predictions regarding the total star population and the relative contributions from several different galaxy components. For this run, the "Asymmetric" component is turned off.

In order to study stars associated with the thick disk, a first order approach would be to cut on the peak of the left lobe. It obviously removes mostly disk stars from the sample, leaving a mix of thick disk and halo stars. We use a truncated median approach with some human interaction to guide the result. A sample determination is given in Figure 6 which covers the same magnitude range as the model predictions in Figure 5.

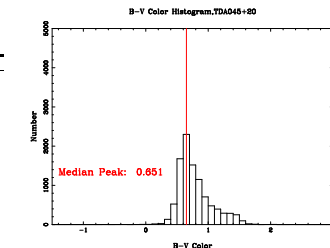


Figure 6. Color histogram for stars between $V = 16$ and $V = 19$ in our field, showing the location of the determined peak color.

The final task is to estimate the completeness of each field. Classically in a Euclidean Universe, completeness is determined by making a plot of magnitude vs. the log of the differential number of counts and determining the magnitude at which the cumulative counts predicted follow power law. This does not work here since the disk stars are an exponentially decaying density function. We instead adopt a GALM0D-based estimate of completeness. In Figure 7, we show the logarithm of the cumulative number of counts as a function of magnitude for our data (light blue line). The best fit power law between 16th and 19th magnitudes for a Euclidean Universe is shown as a magenta line and a model-based prediction of how the cumulative distribution should appear is plotted in Orange. Completeness limits are determined where the predictions deviate by 0.1 dex from the data after 16th magnitude.

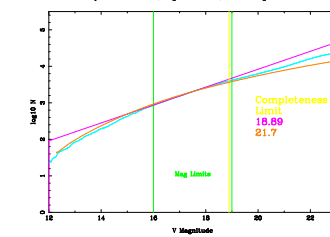


Figure 7. Distribution of project fields on the sky.

Armed with our completeness limits and performing an extinction correction using the maps of Schlegel (1998) we present the number of stars in the indicated magnitude ranges for each of the project fields which lie blueward of the peak B-V color ($(B - V)_p$). The results of these counts are presented in Table 2. Finally, we compute ratios of the observed counts between symmetric pairs of fields in Table 3, along with predictions of what the ratios should be due to the Sun's position above the Galactic midplane using GALM0D.

Table 2. Star Counts from the Thick Disk Asymmetry Project.

Field Name	Area	V_2^a	$(B - V)_p^b$	$16 < V < 19$	$17 < V < 18$	$18 < V < 19$
TDA045+20	1.02	21.0	0.65	3944	1465	1671
TDA050+31	1.02	20.7	0.70	1297	465	509
TDA055+42	1.02	20.5	0.65	632	185	293
TDA060+20	1.00	21.0	0.70	2500	915	985
TDA065+31	1.01	20.5	0.70	946	345	338
TDA075+20	1.02	21.0	0.66	2105	718	779
TDA315+20	0.92	19.0	0.59	3121	1065	1506
TDA310+31	0.91	19.2	0.59	944	319	429
TDA305+42	1.01	20.0	0.69	621	202	277
TDA300+20	0.92	19.0	0.60	2226	820	952
TDA295+31	0.89	19.0	0.58	828	281	361
TDA285+20	0.92	19.0	0.65	1889	670	735
TDA045-20	1.02	21.0	0.70	3479	1241	1513
TDA050-31	1.02	21.0	0.64	1151	391	489
TDA060-20	1.02	21.0	0.68	3016	1063	1171
TDA315-20	0.94	19.0	0.58	3402	1132	1636
TDA300-20	0.96	18.5	0.60	2841	1124	946

Table 3. Blue Peak Ratios for the Thick Disk Asymmetry Project. For the GALM0D Predictions, most fields are on symmetric lines of sight so the model predicts the same number of stars per square degree. The only fields which are an exception to this are the fields which compare counts above and below the plane.

Field Ratio	h_1/h_2	b_1/b_2	GALM0D Ratio Predictions			Observed Count Ratios		
			$16 < V < 19$	$17 < V < 18$	$18 < V < 19$	$16 < V < 19$	$17 < V < 18$	$18 < V < 19$
Quadrant 1/Quadrant 4 ratios above the Galactic Plane								
TDA045+20/TDA315+20	45/315	+20/+20	1.00	1.00	1.00	1.14 ± 0.04	1.21 ± 0.05	1.00 ± 0.05
TDA050+31/TDA310+31	50/310	+31/+31	1.00	1.00	1.00	1.22 ± 0.08	1.28 ± 0.09	1.08 ± 0.09
TDA055+42/TDA305+42	55/305	+42/+42	1.00	1.00	1.00	1.02 ± 0.08	0.98 ± 0.11	0.99 ± 0.11
TDA060+20/TDA300+20	60/300	+20/+20	1.00	1.00	1.00	1.03 ± 0.04	1.01 ± 0.07	0.93 ± 0.06
TDA065+31/TDA295+31	65/295	+31/+31	1.00	1.00	1.00	1.01 ± 0.07	1.07 ± 0.11	0.82 ± 0.09
TDA075+20/TDA285+20	75/285	+20/+20	1.00	1.00	1.00	1.01 ± 0.04	0.97 ± 0.07	0.96 ± 0.07
Quadrant 1/Quadrant 4 ratios below the Galactic Plane								
TDA045-20/TDA315-20	45/315	-20/-20	1.00	1.00	1.00	0.94 ± 0.03	1.01 ± 0.06	0.87 ± 0.04
TDA060-20/TDA300-20	60/300	-20/-20	1.00	1.00	1.00	1.00 ± 0.04	0.89 ± 0.05	1.17 ± 0.07
Quadrant 1 ratios above/below the Galactic Plane								
TDA045+20/TDA045-20	45/45	+20/-20	0.94	0.94	0.97	1.13 ± 0.04	1.18 ± 0.06	1.10 ± 0.05
TDA050+31/TDA050-31	50/50	+31/-31	0.97	0.97	0.98	1.13 ± 0.04	1.17 ± 0.11	1.04 ± 0.09
TDA060+20/TDA060-20	60/60	+20/-20	0.94	0.93	0.96	0.90 ± 0.05	0.86 ± 0.06	0.84 ± 0.05
Quadrant 4 ratios above/below the Galactic Plane								
TDA315+20/TDA315-20	315/315	+20/-20	0.94	0.94	0.97	0.94 ± 0.04	0.94 ± 0.06	0.92 ± 0.05
TDA300+20/TDA300-20	300/300	+20/-20	0.94	0.93	0.96	0.82 ± 0.05	0.73 ± 0.04	1.00 ± 0.07



We would like to thank the NSF for financial support, NOAO for observing support, and our respective home institutions for providing facilities support.